AGU PUBLICATIONS

JGR

Journal of Geophysical Research: Atmospheres

RESEARCH ARTICLE
10.1002/2017JD027208

Key Points:
- Monthly mean fine dust levels display large-scale covariability across the western U.S. during 2002–2015 on interannual time scales
- Key drivers of fine dust interannual variability are regional precipitation and soil moisture, and trans-Pacific transport of Asian dust
- Recent increase in Southwest fine dust levels in March are associated with changes in regional hydroclimate and trans-Pacific transport

Supporting Information:
- Supporting Information S1

Correspondence to:
P. Achakulwisut,
pachakulwisut@fas.harvard.edu

Citation:
Achakulwisut, P., Shen, L., & Mickley, L. J. (2017). What controls springtime fine dust variability in the western United States? Investigating the 2002–2015 increase in fine dust in the U.S. Southwest. *Journal of Geophysical Research: Atmospheres*, *122*, 12,449–12,467. https://doi.org/10.1002/2017JD027208

Received 26 MAY 2017
Accepted 27 OCT 2017
Accepted article online 3 NOV 2017
Published online 18 NOV 2017

©2017. American Geophysical Union. All Rights Reserved.

What Controls Springtime Fine Dust Variability in the Western United States? Investigating the 2002–2015 Increase in Fine Dust in the U.S. Southwest

Pattanun Achakulwisut[1], Lu Shen[2], and Loretta J. Mickley[2]

[1]Department of Earth and Planetary Sciences, Harvard University, Cambridge, MA, USA, [2]School of Engineering and Applied Sciences, Harvard University, Cambridge, MA, USA

Abstract We use empirical orthogonal function (EOF) analysis to investigate the role of meteorology in controlling the interannual variability of fine dust concentrations in the western United States during 2002–2015 March–May. We then develop a prediction model to explore the causes of an observed increase in fine dust concentrations during March in the Southwest. For each spring month, 54–61% of the total variance in fine dust anomalies can be explained by the first two leading EOF modes, which consist of a coherent pattern of covariability across the West and a dipole northwest-southwest pattern. We identify the key meteorological controlling factors to be regional precipitation, temperature, and soil moisture, which are in turn mostly driven by large-scale changes in sea surface temperature and/or atmospheric circulation patterns, including the El Niño–Southern Oscillation (ENSO) and Pacific Decadal Oscillation (PDO). In addition, fluctuations in the trans-Pacific transport of Asian dust likely contribute to fine dust variability in March and April. We find that March fine dust concentrations have increased from 2002 to 2015 in the Southwest (0.06 ± 0.04 μg m^{-3} a^{-1}, $p < 0.05$). Multiple linear regression analysis suggests that these increases are associated with the following: (1) regionally drier and warmer conditions driven by constructive interference between ENSO and PDO, (2) soil moisture reductions in areas spanning the North American deserts, and (3) enhanced trans-Pacific transport. Our results provide an observational basis for improving dust emission schemes and for assessing future dust activity under climate change.

Plain Language Summary Soil-derived particulate matter, also known as mineral dust, contributes to air quality degradation, visibility reduction, and public health risks in the western United States, where abundant arid lands serve as dust sources. Dust is also transported here from Asian deserts across the Pacific Ocean. Improved understanding of how meteorology influences airborne dust levels in the present day can help us assess future changes due to human-caused climate change. Using statistical methods, we identify the key drivers of year-to-year changes in springtime dust across the West to be regional precipitation, temperature, and soil moisture. These drivers are in turn influenced by the El Niño–Southern Oscillation (ENSO) and Pacific Decadal Oscillation (PDO). Trans-Pacific transport of Asian dust also contributes to the observed dust variations. We find that dust levels have been increasing in southwestern regions between 2002 and 2015. This increase is associated with (1) regionally drier and warmer conditions associated with ENSO and PDO, (2) declines in soil moisture across North American deserts, and (3) stronger transport of Asian dust. With the U.S. Southwest projected to experience severe and persistent droughts in coming decades due to climate change, our results suggest that this region could also become increasingly dustier.

1. Introduction

Air quality is strongly influenced by meteorological conditions, and there are growing concerns that climate change could enhance mineral dust mobilization and transport across the western United States. Recent studies suggest that deposition of atmospheric dust and its concentrations may have been increasing in the West over the past two decades (Brahney et al., 2013; Hand et al., 2016). Yet relatively few studies have examined the relationships between meteorology and mineral dust aerosol loading in the United States. Those that have are mostly limited in terms of spatial domain, temporal scale, and/or meteorological variables considered. In this study, we perform a systematic statistical analysis to (1) investigate the role of meteorology in controlling the interannual variability of fine dust concentrations across the western U.S. during the spring months and (2) examine the causes of a recent increase in fine dust concentrations in the

Southwest in March. Our study relies on a 14 year record (2002–2015) of observed concentrations of fine dust, defined as soil-derived particulate matter smaller than 2.5 μm aerodynamic diameter ($PM_{2.5}$). With the Southwest projected to become drier and hotter in the coming decades due to human-caused climate change (e.g., Ault et al., 2016; Cook et al., 2015; Seager & Vecchi, 2010), our work has important public health and socioeconomic implications for the region.

Data from ground-based monitoring sites between 2001 and 2014 indicate that surface fine dust concentrations increase abruptly over much of the western U.S. each spring (Hand et al., 2017; Malm et al., 2004). Such broad-scale regional and temporal behaviors are indicative of influence by large-scale emission and transport mechanisms. In southwestern regions, the spring months are a period of higher, sustained wind speeds and lower precipitation (Flagg et al., 2014), and monthly mean fine dust concentrations can contribute up to ~50% to total $PM_{2.5}$ (Hand et al., 2017). Large dust storms, spanning up to 160 km wide and several kilometers high, are a common phenomenon in the spring (Bach & Brazel, 1996; Idso et al., 1972; Lei & Wang, 2014). Dust is generated by wind erosion of exposed soils and by human activities such as construction, agricultural operations, and travel on unpaved roads (Mansell et al., 2007). The Mojave, Great Basin, Sonoran, and Chihuahuan Deserts are the major sources of dust in North America (Jewell & Nicoll, 2011; Reynolds et al., 2007; Rivera Rivera et al., 2010; Tanaka & Chiba, 2006). Land disturbance of the semiarid Columbia Plateau, Colorado Plateau, and southern Great Plains—primarily through agriculture and fossil fuel development—have also made these regions active dust sources (Carmona et al., 2015; Neff et al., 2008; Saxton et al., 2000; Skiles et al., 2015; Reynolds et al., 2016). Sediment records suggest that the anomalously high dust deposition rates in the western U.S. over the past 3,000–5,000 years are associated with droughts, land disturbance, and livestock grazing (Brahney et al., 2013; Neff et al., 2008; Routson et al., 2016). It is also well established that dust originating from the deserts of Mongolia and northern China can be transported across the Pacific Ocean and contribute to the total dust burden across the West, especially in the Pacific Northwest and coastal California regions (e.g., Creamean et al., 2014; Fairlie et al., 2007; Fischer et al., 2009; Kavouras et al., 2009; VanCuren & Cahill, 2002; Zhao et al., 2006). This trans-Pacific transport is most active during spring, when extratropical cyclone activities and midlatitude westerlies are strongest (Yu et al., 2008). During this season, the potential for wet deposition of dust over the Pacific Ocean during transport is also relatively low (Creamean et al., 2014). However, the mass of Asian dust transported to the western United States is not well quantified. For example, Yu et al. (2012) estimated that 56 megaton (Mt) (40% of total export) of Asian dust transported reaches the western United States each year, whereas Zhao et al. (2006) estimated this value to be 3.6 Mt (3%).

Mineral dust aerosols have far-reaching effects on climate, ecosystems, and humans. Atmospheric dust affects the Earth's energy budget through aerosol-radiation and aerosol-cloud interactions (Carslaw et al., 2010; Miller et al., 2014) or by decreasing the albedo of snow and ice when deposited on such surfaces, causing earlier and faster snowmelt and river runoff (Painter et al., 2007, 2010). Deposited dust also influences biogeochemical cycles in oceans and on land, including fertilization of terrestrial and marine ecosystems (Jickells, 2005). Dust episodes can also contribute to declines in air quality, visibility, and agricultural productivity (Middleton, 2017). In the western United States, severe dust storms can raise PM levels far above the National Ambient Air Quality Standards and have been found to be associated with premature mortality (e.g., Crooks et al., 2016; Kavouras et al., 2007; Raman et al., 2014). In addition, an array of allergens, pathogens, and toxic chemicals may be carried by airborne dust. Such constituents, along with soil particles, can cause or aggravate respiratory and cardiovascular disorders, conjunctivitis, and skin irritations (Goudie, 2014; Kim et al., 2015; Plumlee & Ziegler, 2007). In the Southwest, there are growing public health concerns that higher airborne dust levels could in particular lead to increased exposure of (1) toxic contaminants from landfills and abandoned or active mines (Csavina et al., 2012) and (2) soil-borne fungi, *Coccidioides* spp., known to live in the desert Southwest soils which, when inhaled, can cause Valley Fever (Schneider et al., 1997). Since the late 1990s, the incidence of Valley Fever in the Southwest has risen by a factor of 8, but whether the increase is related to greater awareness of the disease, increased population of susceptible individuals or to an enhancement in airborne dust is not yet known (Tsang et al., 2013).

Previous studies suggest that airborne dust levels may have been increasing in the western United States over the past few decades. Brahney et al. (2013) found that atmospheric calcium deposition increased between 1994 and 2009 across the intermountain west, midwest, and northwest regions. The authors concluded that the most likely cause is enhanced dust emission arising from increases in aridity, high wind

events, and anthropogenic disturbance of soils. Hand et al. (2016) reported that springtime fine dust concentrations have increased from 1995 to 2014 across the Southwest, primarily in March (5.4% a^{-1}, $p < 0.01$). Trends in April and May were not as high or regionally extensive. The authors suggest that the regional increase in March is primarily due to two factors: (1) an earlier onset of the spring dust season and (2) a shift of the March Pacific Decadal Oscillation (PDO) to the negative phase, which resulted in drier, winder, and less vegetated conditions across the Southwest.

Dust emission schemes in dynamic, three-dimensional models currently vary widely in complexity and approach, resulting in large intermodel differences in simulated dust fluxes (e.g., Huneeus et al., 2011; Uno et al., 2006). Better understanding of wind erosion processes and of the relationships between airborne dust and meteorological variables will allow us to improve dust emission schemes (Webb et al., 2016), as well as provide an observational foundation for rapid assessment of future dust activity under a range of climate change scenarios. To date, relatively few studies have attempted to rigorously characterize observed relationships of meteorological variables and mineral aerosols, especially across a large spatial domain or on multiyear time scales. For example, using total PM_{10} as a dust proxy, Csavina et al. (2014) observed a dependence of dust concentrations on relative humidity at wind speeds greater than 4 m s^{-1} across eight sites in Arizona and Mexico in 2011 March–May. Focusing on episodic dust storm events in Salt Lake City, Utah, Hahnenberger and Nicoll (2012) found that such events are mostly caused by approaching midlevel troughs, resulting in strong southwesterly winds that entrained sediments upwind.

In this study, we seek to answer two overarching questions. First, do fine dust concentrations across the western United States display broad-scale spatial behaviors and correlations to meteorology on interannual time scales? Second, what are the underlying causes of an increase in March fine dust concentrations between 2002 and 2015 in the Southwest? To answer the first question, we apply empirical orthogonal functions (EOFs) to decompose the interannual variability of monthly mean fine dust concentrations in the western United States for a 14 year record of observations (2002–2015) for each of the spring months (March–May). We then perform a systematic correlation analysis between the first two leading EOF modes and an array of variables to identify key meteorological controlling factors. To answer the second question, we develop statistical models by regressing potential meteorological predictors identified by EOF-correlation analyses onto fine dust concentration time series.

2. Data and Methods

2.1. Fine Dust Data

We rely on ground-based measurement data from the Interagency Monitoring of Protected Visual Environments (IMPROVE) network to calculate fine dust concentrations for the 2002–2015 period (Malm et al., 1994). The locations of IMPROVE sites in the western United States (31°–49°N, 100°–125°W) are shown in Figure 1. The IMPROVE network began operation in 1988 with 20 sites and expanded to 165 sites between 2000 and 2003, with the majority of sites located in remote and rural locations (Malm et al., 2004). Since Empirical Orthogonal Function (EOF) analysis requires no missing data, we restrict our analyses to the years 2002–2015 and include only those sites with at least 7 years of monthly data over the 14 year period. This leads to 91 sites with less than 8% of missing monthly data.

We follow the approach of Hand et al. (2016) in using the iron content of filter samples as a fine dust proxy with some modifications. We calculate monthly mean fine dust concentrations as follows: (1) We neglect any sites at which $PM_{2.5}$-Iron is measured below the minimum detection limit for more than 20% of the total measurements available during the 14 year period. (2) We screen out "high-combustion" days when the elemental carbon (EC) concentration exceeds a threshold value, defined as the 2002–2015 EC monthly mean + 1 standard deviation for a given site. (3) For each site and month containing at least 50% complete data (i.e., 10 days/month since IMPROVE measurements are made every third day), we calculate monthly mean $PM_{2.5}$-Iron concentrations from daily values. (4) We approximate monthly mean fine dust concentrations as $PM_{2.5}$-Iron/0.058, based on observed linear relationships between daily $PM_{2.5}$-Iron and IMPROVE "Fine Soil" from 2011 to 2015 (Figure S1 in the supporting information). The analytical uncertainties associated with our calculated monthly mean fine dust values are ~0.05% on average (maximum ~3%) by error propagation. We discuss in the supporting information our reasons for focusing on fine dust and further details in using and validating $PM_{2.5}$-Iron as a fine dust proxy (section S1). Although IMPROVE measurements are made

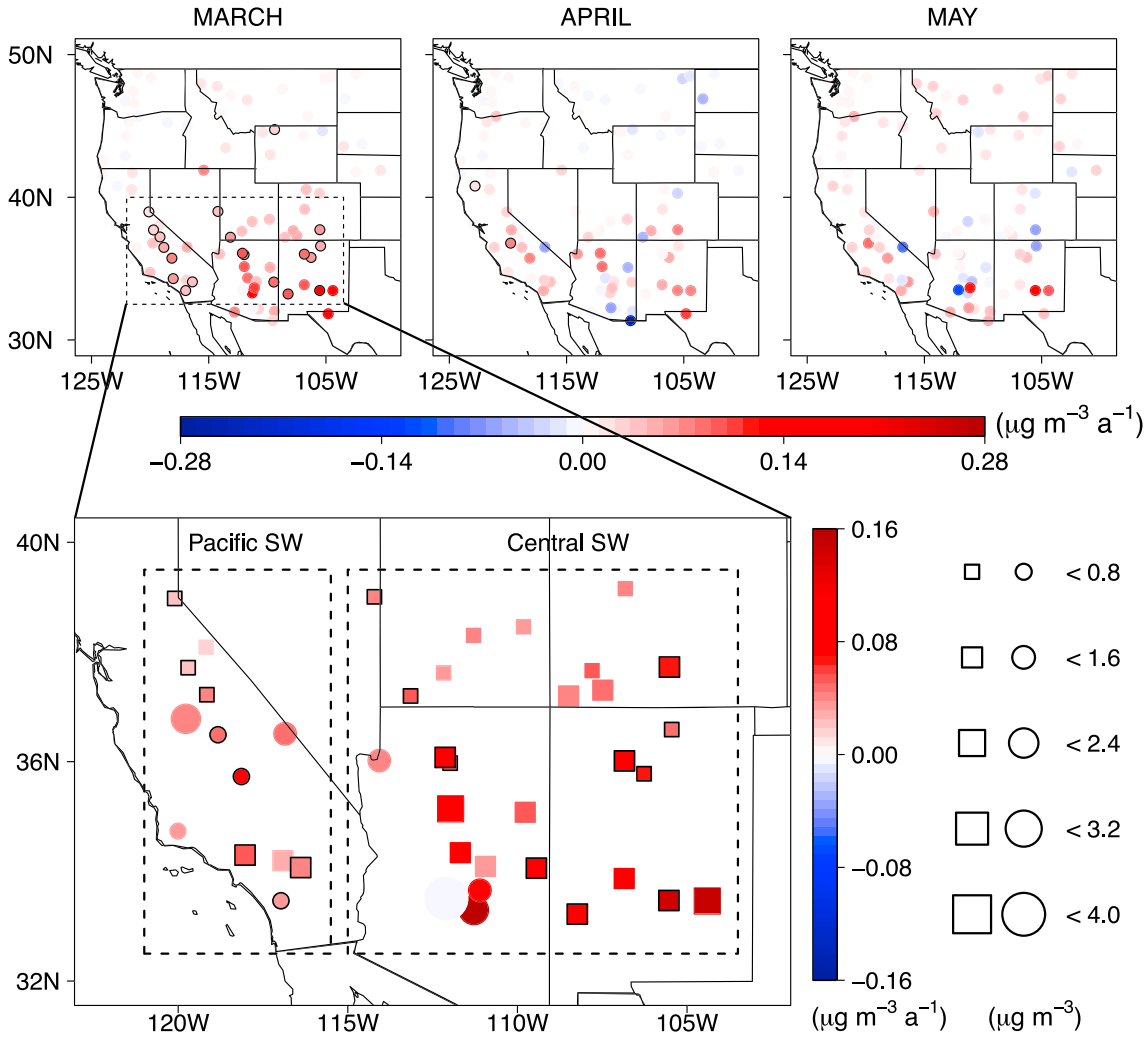

Figure 1. (top) Trends of monthly mean fine dust concentrations from 2002 to 2015 in the spring at IMPROVE network sites across the western United States (31°–49°N, 100°–125°W). Symbols with black outlines denote sites with statistically significant trends ($p < 0.05$). Fine dust is derived from $PM_{2.5}$-Iron. (bottom) A close-up for March for sites located between 33°–39.5°N and 103°–121°W. Symbol color shows the trend and symbol size scales with the 2002–2015 average concentration as indicated. Circles correspond to sites with elevations at or below 1,000 m above sea level (asl); squares correspond to those with elevations greater than 1,000 m asl. Symbols with black outlines denote sites with statistically significant trends ($p < 0.05$). The boxes outline two different domains used to calculate regional means in Figure 5: Pacific Southwest (33°–39.5°N, 115.5°–121°W) and Central Southwest (33°–39.5°N, 103°–115°W). The large pale blue dot in southern Arizona represents the average value at two sites in Phoenix.

every third day, the 2002–2015 monthly mean time series appear to capture the frequency of extreme dust events to some extent (section S2 and Figure S2). We find that the 2002–2015 trends in monthly mean fine dust concentration across the western United States are not sensitive to the threshold EC value in step 2 (section S3 and Figure S3).

2.2. Meteorological Data and Standard Climate Indices

In our EOF-correlation analysis (section 2.4), we consider a wide range of meteorological variables and standard climate indices that are likely to influence dust activity across the western United States (Table S1). Monthly total precipitation (rain + snow), mean surface temperature (T_{mean}), and maximum surface temperature (T_{max}) for the contiguous United States are from the Parameter-elevation Regression on Independent Slopes Model (PRISM) Climate Group, regridded from 4 km × 4 km to 0.2° × 0.2° (Oregon State University, http://prism.oregonstate.edu). Monthly mean sea level pressure, wind velocity, geopotential height, and relative humidity are from the National Centers for Environmental Prediction-Department of Energy Reanalysis II

at 2.5° × 2.5° (Kanamitsu et al., 2002). For wind velocity, we also use 0.5° × 0.625° reanalysis data from the Modern-Era Retrospective analysis for Research and Applications, Version 2 (Gelaro et al., 2017). Sea surface temperatures (SSTs) come from the National Oceanic and Atmospheric Administration (NOAA) Extended Reconstructed Sea Surface Temperature 2° × 2° data set (NOAA_ERSST_V4, http://www.esrl.noaa.gov/psd/). For geopotential height, wind speed, and relative humidity, data at pressure levels of 1,000, 750, 500, and 250 mb are considered in our correlation analysis. All other variables are surface data. We apply grid-box-area-weighting to calculate regional averages from gridded data.

We use the following standard climate indices: (1) Western Pacific (WP), (2) Pacific/North American (PNA), (3) El Niño–Southern Oscillation Oceanic Niño Index (ENSO ONI), and (4) Pacific Decadal Oscillation (PDO). The first three are from the NOAA Climate Prediction Center. The WP and PNA monthly indices describe atmospheric teleconnection patterns derived from 500 mb geopotential height anomalies in the Northern Hemisphere. The ENSO ONI captures the 3 month running mean SST anomalies in the Niño3.4 region (5°N–5°S, 120°–170°W), based on centered 30 year base periods updated every 5 years. The PDO index is from the Joint Institute for the Study of the Atmosphere and Ocean (Mantua et al., 1997) and is derived as the leading principal component of monthly SST "anomaly deviations" in the North Pacific Ocean, poleward of 20°N. Anomaly deviations—that is, departures of local SST anomalies from the concurrent global mean SST anomaly—distinguish this pattern of variability from the signal of global warming.

We also use the gridded 0.5° × 0.5° monthly Standardized Precipitation-Evapotranspiration Index (SPEI, v2.5) from the Spanish National Research Council (CSIC, Vicente-Serrano et al., 2010). The SPEI uses monthly precipitation and potential evapotranspiration values from the Climatic Research Unit of the University of East Anglia (CRU TS data set version 3.23) to determine the water balance, which can be aggregated over different time scales to monitor drought conditions in different hydrologic subsystems. Short time scales are mainly related to soil water content and river discharge in headwater areas, medium time scales are related to reservoir storages and discharge in the medium course of rivers, and long time scales are related to variations in groundwater storage. In our analysis, SPEI values aggregated over 1, 3, 6, 12, and 48 months are considered. We chose the SPEI as a drought index in our analysis for two reasons. First, it takes into account both precipitation and potential evapotranspiration in determining drought conditions. Second, its multiscalar characteristics enable representation of drought conditions in different hydrologic subsystems.

Springtime satellite retrievals of 550 nm aerosol optical depth (AOD) from Moderate Resolution Imaging Spectroradiometer (MODIS) Dark Target are also used to corroborate our findings.

2.3. Trend Analysis

The Mann-Kendall test is used to assess the statistical significance of a monotonic trend, and the Theil-Sen estimator is used to calculate the slope of the trend. The Mann-Kendall test is a nonparametric test for a monotonic trend (Sen, 1968), which is more robust to outliers than regression. Likewise, the Theil-Sen estimator is a nonparametric alternative to the parametric ordinary least squares regression line. Trends derived using the Theil-Sen method take into account how the median value across an ensemble of samples changes linearly with time. Only sites with at least 7 years of monthly data over the 14 year period are included in trend analyses throughout this study.

2.4. Empirical Orthogonal Function and Correlation Analyses

We examine the spatial patterns of fine dust interannual variability in the western United States through EOF analysis. This method is commonly used in climate and atmospheric research to analyze fields with high spatiotemporal dimensionality (Taylor et al., 2013). In this case, we use a data matrix $\mathbf{S}$ ($n \times p$) to represent the standardized anomalies of monthly mean fine dust concentrations in the West over n monthly time steps and p sites. We construct $\mathbf{S}$ for each of the spring months (March–May) as follows. First, the 2002–2015 time series of monthly mean fine dust concentrations for each site is detrended by subtracting the linear trend obtained by simple linear regression and standardized by the 2002–2015 standard deviation of each site. We detrend the data to focus on interannual variability, and we standardize the data because IMPROVE sites are located at a wide range of elevations and distances to urban centers and display different standard deviations (Figure S4a). Second, to fill in any missing values in the data matrix, we use the method of Data Interpolating Empirical Orthogonal Functions (Alvera-Azcárate et al., 2005; Beckers & Rixen, 2003). This

iterative EOF-based interpolation method has been shown to be a superior approach in terms of reconstruction accuracy (Taylor et al., 2013). Lastly, we perform EOF analysis via covariance matrix decomposition. The temporal covariance between different sites can be written mathematically as $\mathbf{A} = \mathbf{S}^T\mathbf{S}/(n-1)$. The EOF spatial loadings are given by the eigenvectors of **A**, and the corresponding eigenvalues reflect the portion of total variance explained by each EOF. The principal components (PCs), which describe how the amplitude of each EOF varies with time, are derived by projecting **S** onto the eigenvectors of **A**.

Because we are interested in the role of large-scale meteorology and climate variability on fine dust activity, we examine the correlations of each EOF spatial pattern with key parameters for a range of multiple time frames, as discussed in section 2.2 and listed in Table S1. Meteorological variables are detrended but not standardized. We use two common data visualization methods to interpret the EOF analysis results: (1) homogeneous correlation maps, which display the statistically significant correlation between the principal component time series of a given EOF mode (*k*th PC) and the site-specific time series of standardized anomalies in monthly mean fine dust; and (2) heterogeneous correlation maps, which provide the statistically significant correlation between the *k*th PC and the detrended time series of a particular meteorological variable at each grid box. We note here that in some cases the dust PCs show strong spatial correlations with both monthly maximum and mean surface air temperatures. However, the correlations between a given PC and maximum temperature tend to yield a more extensive spatial pattern than those for mean temperature, providing a clearer picture of the regional-scale influence. We thus choose to display maximum temperature in our figures.

2.5. Multiple Linear Regression Analysis

In this analysis, we use linear forward stepwise regression to develop empirical relationships between observed regional fine dust concentrations and a set of meteorological variables and standard climate indices. Meteorological data are not detrended in this analysis. We use four selection criteria in our stepwise regression. First, the chosen parameter must lead to a model with the lowest value of the Bayesian Information Criterion (BIC). Based on the maximum likelihood estimates of the model parameters, the BIC is defined in multiple regression as $n + n\log(2\pi) + n\log(\mathrm{RSS}/n) + \log(n)(p+1)$, where n is the number of observations, RSS is the residual sum of squares, and p is the number of parameters. Second, the selected parameters must be independent of each other. We minimize multicollinearity by testing that the Variance Inflation Factor (VIF) of the selected parameters does not exceed a significant threshold value of 10 (Kutner et al., 2004). VIF, a widely used index of collinearity in regression analysis, is defined as $1/\left(1-R_k^2\right)$, where R_k^2 is the coefficient of multiple determination obtained by regressing the *k*th predictor on the remaining parameters. Third, the adjusted coefficient of multiple determination, R^2, of each new model in the stepwise process must be greater than the previous one by at least 0.05. Fourth, given that we have only 14 years of data, no more than three variables can be selected to avoid overfitting. Section S5 of the supporting information describes more details of the validation of the multiple linear regression models.

Unless otherwise specified, we use $p < 0.05$ as the threshold for statistical significance.

3. Results

3.1. Trends in Springtime Fine Dust Concentrations in the Western United States

We first investigate trends in surface monthly mean fine dust concentrations in the western United States during the spring months (March–May) from 2002 to 2015. As Figure 1 shows, there is a north-south contrast in which most sites located south of 40°N display increasing trends in March over the 14 year period, whereas sites north of 40°N show smaller increasing or, in some cases, decreasing trends. Out of the 50 sites located south of 40°N, 19 display statistically significant trends, as denoted by symbols with black outlines. Conversely, there is a less coherent pattern for April and May, with few to no sites showing statistically significant trends. Trend analysis performed with normalization displays similar spatial patterns (Figure S4b). During spring, sites located in the Southwest experience the largest variability in monthly mean fine dust concentrations (Figure S4a).

Based on these results and those of Hand et al. (2016), we consider trends in monthly mean rather than seasonal mean in order to determine meteorological drivers of the statistically significant and regionally extensive increases in fine dust concentrations across the Southwest in March. Moreover, precipitation,

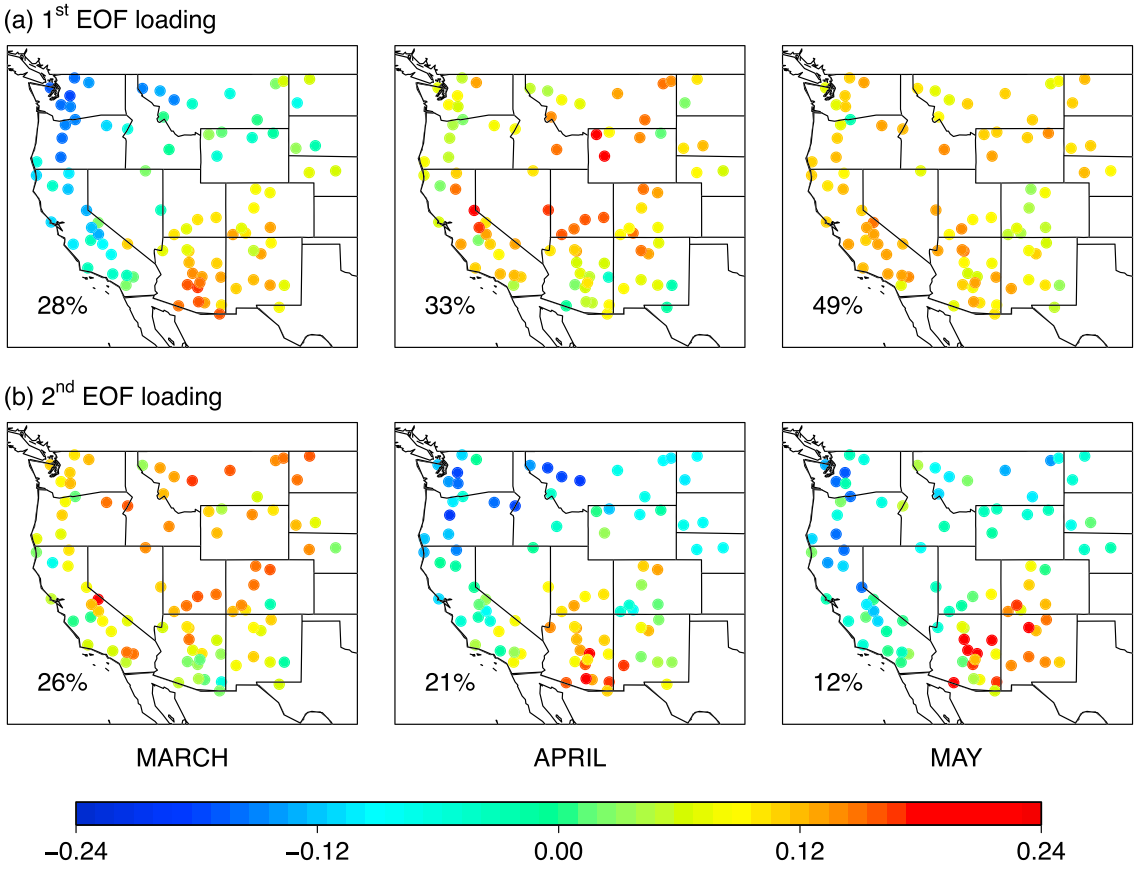

Figure 2. EOF loadings of standardized anomalies of monthly mean fine dust concentrations for 2002–2015 March–May. For each month, the first EOF mode is shown in the top row and the second EOF mode is shown in the bottom row. The percentage of total variance explained by each EOF mode for a given month is displayed inset.

which plays a potentially important role in controlling dust variability (Elmore et al., 2008), displays large intermonthly spatial differences across the West during spring (Guirguis & Avissar, 2008; Mock, 1996).

3.2. Interannual Variability of Springtime Fine Dust Concentrations and Meteorological Covariates

Using EOF analysis, we identify the dominant spatial patterns of fine dust interannual variability in the western United States from 2002 to 2015 and their meteorological covariates. We find that in each spring month, over half (54–61%) of the total variance is captured by the first two leading EOF modes, which display in-phase covariability across most sites in the western United States or a Northwest-Southwest dipole of variability (Figure 2). Such broad-scale behaviors are indicative of influence by large-scale controlling mechanisms.

Figure 3 shows the EOF-correlation analysis results for the first EOF mode (EOF1) for March, which explains 28% of the total variance. Figure 3a shows the principal component time series associated with this pattern (PC1), and Figure 3b shows the homogeneous correlation map, displaying a Northwest-Southwest dipole of variability. Consistent with Creamean et al. (2014), fine dust measured at high-elevation mountain sites in California vary coherently with those in the Pacific Northwest. We find that PC1 is significantly correlated to the 3 month running mean of three standard climate indices during late summer of the previous year through the early spring of the current year, especially for the current-year January–March (JFM) months. The three indices are ENSO ONI ($r = -0.74$; shown in Figure 3a), PDO ($r = -0.66$; shown in Figure 3a), and PNA ($r = -0.58$; not shown). These correlations are consistent with the heterogeneous correlation plot between PC1 and JFM SST anomalies (Figure 3c), which shows statistically significant correlations in regions of the Pacific Ocean associated with ENSO (SST anomalies in the Niño3.4 region, 5°N–5°S, 120°–170°W) and PDO (horseshoe pattern of anomalies, in which SSTs along the equator in the eastern-central Pacific and coast of western North America are opposite in sign to those in the north-central Pacific Ocean). In addition, the

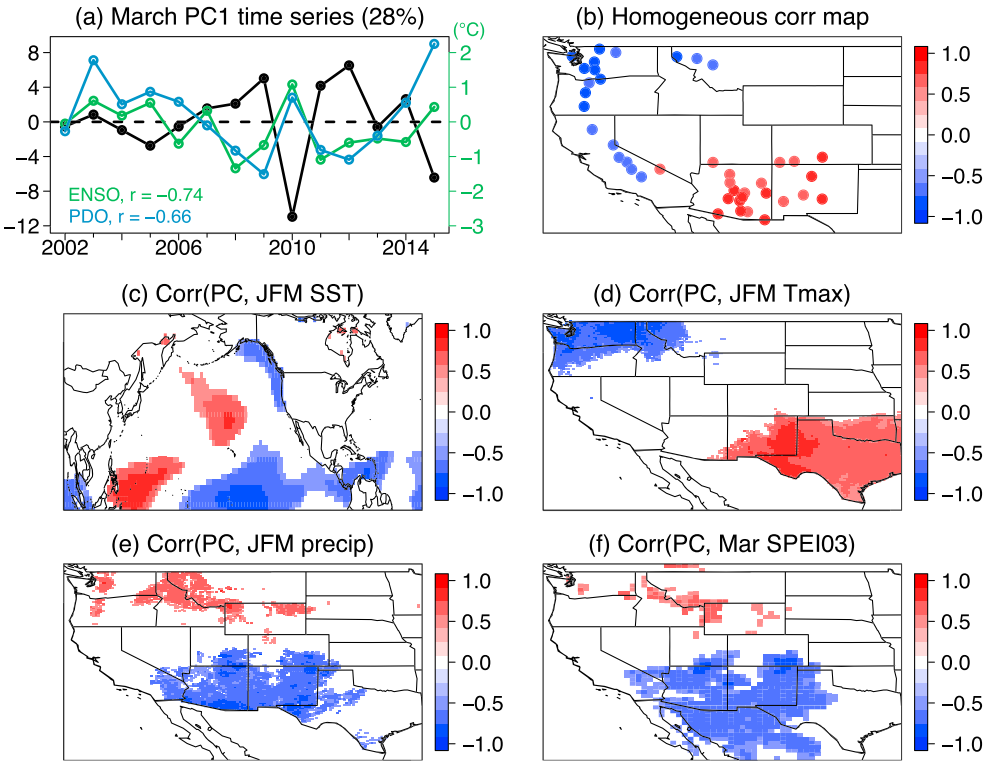

Figure 3. Analysis of the first EOF mode of standardized monthly anomalies of March fine dust concentrations between 2002 and 2015, which explains 28% of the total variance. (a) Time series of the principal components of the first EOF mode ("PC1," black). The panel also shows the time series of current-year JFM El Niño–Southern Oscillation (ENSO) ONI index (green) and current-year JFM Pacific Decadal Oscillation (PDO) index (blue). Correlations of these indices with March PC1 are shown inset. The left axis corresponds to PC1 values and the right to the ENSO ONI and PDO indices. (ONI values have units of °C whereas PDO values are unitless.) (b) Homogeneous correlation map between PC1 and the time series of standardized monthly fine dust anomalies at IMPROVE sites. Panels in the two rows below show heterogeneous correlation maps between PC1 and current-year JFM (c) mean sea surface temperatures (SST), (d) maximum surface air temperature (T_{max}), and (e) total precipitation, and (f) March 3-month Standardized Precipitation-Evapotranspiration Index (SPEI03). In Figures 3b–3f, only those sites or grid cells with statistically significant correlations ($p < 0.05$) are shown. Monthly meteorological variables are detrended but not standardized.

correlation maps between PC1 and maximum air temperature (Figure 3d) and total precipitation (Figure 3e) display distinctive Northwest-Southwest dipole patterns that are characteristic of those associated with ENSO and PDO (e.g., Seager et al., 2005; Sheppard et al., 2002; Weiss et al., 2009). The correlation map between PC1 and March 3-month Standardized Precipitation-Evapotranspiration Index (SPEI03) also reveals a Northwest-Southwest dipole pattern. The correlation pattern in the south encompasses regions of the Mojave, Sonoran, and Chihuahuan Deserts, which are important sources of natural dust for the southwest United States (Reynolds et al., 2007; Rivera Rivera et al., 2010). The 3-month SPEI is often used as a proxy for soil moisture (Herold et al., 2016; Törnros & Menzel, 2014).

These findings suggest that this Northwest-Southwest dipole pattern of fine dust covariability is driven by anomalies in regional precipitation, temperature, and soil moisture, which are in turn influenced by natural variability in the North Pacific sea surface temperatures. As described by Seager et al. (2003, 2005) and Weiss et al. (2009), El Niño conditions are associated with a southward shift of the Pacific storm track, increasing winter precipitation across the southern United States. In the Northwest, enhanced flow of marine air into the Northwest along with reduced northerly flow of cold air from Canada leads to above-average temperatures. Conversely, La Niña conditions are associated with increased high-pressure blocking activity over the eastern North Pacific and a subtropical jet stream that is weaker and more poleward. This pattern induces subsidence over the Southwest and increases precipitation and frequency of cold-air outbreaks in the Northwest. Constructive interference between interannual ENSO and decadal-to-multidecadal PDO

variability can amplify the impacts of ENSO (Wang et al., 2014; Weiss et al., 2009). Between 2002 and 2015, JFM ENSO and PDO were significantly correlated ($r = 0.69$), suggesting that the ENSO-related meteorological patterns were intensified by PDO during this period. In addition, results from a model study by Gong et al. (2006) suggest that ENSO also modulates the trans-Pacific transport of Asian dust. El Niño years are associated with a northward shift of the trans-Pacific transport path and positive anomalies in dust loading north of 45°N in the western United States (with negative anomalies to the south).

Given that local and regional domestic sources are the dominant contributors of dust measured at Southwest sites, while Asian dust is the primary contributor at mountain sites located in California and the Pacific Northwest in spring (Creamean et al., 2014; Fairlie et al., 2007; Kavouras et al., 2009), we interpret our results as follows. Positive PC1 years in which fine dust levels are higher than average in the Southwest are generally associated with the following: (1) negative ONI values—that is, La Niña conditions with cool SSTs in the Niño3.4 region, (2) negative PDO values—that is, cool SSTs along the equator in the eastern and central Pacific and coast of western North America and warm SSTs in the north-central Pacific, and (3) negative PNA values—that is, a strong blocking anticyclone over the extratropical North Pacific and below-average geopotential heights over the Intermountain Region of North America. As a result of one or more of these phenomena, the U.S. Southwest and northern Mexico experience drier and warmer conditions, leading to greater dust emissions from domestic sources. For the mountain sites in the Pacific Northwest and California, fine dust is lower than average during positive PC1 years, most likely due to reduced transport of Asian dust and wetter conditions that lead to more efficient scavenging of airborne dust.

Figure 4 shows the EOF-correlation analysis results for the second EOF mode (EOF2) for March, which explains 26% of the total variance. Figure 4a shows the principal component time series associated with this pattern (PC2), and Figure 4b shows the homogeneous correlation map, displaying a coherent pattern of covariability across almost all sites in the western United States. We do not find significant correlations between the PC2 time series and local meteorological variables (precipitation, air temperature, relative humidity, and wind speed). Instead, PC2 is strongly correlated to large-scale midtroposphere atmospheric circulation anomalies that influence trans-Pacific transport of Asian dust. Figure 4c reveals a north-south dipole of 500 mb geopotential height anomalies in the midtroposphere (3–10 km) over the North Pacific Ocean, where trans-Pacific transport peaks (Zhao et al., 2006). This dipole pattern is indicative of an intensified meridional pressure gradient over the central North Pacific, resulting in stronger westerly flows and the likelihood of enhanced dust transport from Asia during positive PC2 years. To quantify the influence of this geopotential height pattern on dust, we define a new metric, the meridional gradient index (MGI), as the difference between the 500 mb geopotential heights averaged over two domains outlined in Figure 4c: 27.5°–42.5°N, 170°E–160°W and 57.5°–67.5°N, 165°E–165°W. The PC2 and detrended March MGI time series are significantly correlated ($r = 0.80$). Since 500 mb geopotential heights decrease with increasing latitude, positive MGI values represent a stronger south-to-north meridional gradient in the midtroposphere over the North Pacific, indicative of stronger westerly flow. As expected, we find a significant correlation ($r = 0.98$) between the detrended March time series of MGI and zonal winds averaged over a domain in between the two pressure centers (42.5°–57.5°N, 170°E–160°W).

The variability of March EOF2 thus appears to be primarily influenced by trans-Pacific transport of Asian dust. As Figure 4a shows, this result is consistent with a significant correlation coefficient ($r = 0.75$) between PC2 and the detrended time series of MODIS satellite retrievals of 550 nm aerosol optical depth (AOD) averaged over a domain in between the two pressure centers (37.5°–47.5°N, 160°E–140°W; outlined by the dashed box in Figure 4c) in March. Satellite retrievals of AOD over the North Pacific Ocean in the spring can be used as a proxy for trans-Pacific transport of Asian dust (e.g., Nam et al., 2010; Yu et al., 2008, 2012).

We find that ENSO variability also exerts an influence over fine dust variability in April and May. For April, EOF2 explains 21% of the total variance and consists of a Northwest-Southwest dipole of variability similar to March EOF1 (Figure S5). We find that the April PC2 is significantly correlated to the February-March (FMA) ENSO ONI ($r = -0.66$). Correlation maps between April PC2 and FMA maximum temperature and April SPEI03 display statistically significant regions primarily in Texas and northern Mexico, though the correlations are less spatially extensive than those for March EOF1. We find that positive PC2 years, during which April fine dust concentrations are higher in the Southwest and lower in the Northwest, are associated with La Niña conditions, and warmer and drier conditions in the Southwest and northern Mexico, whereas the

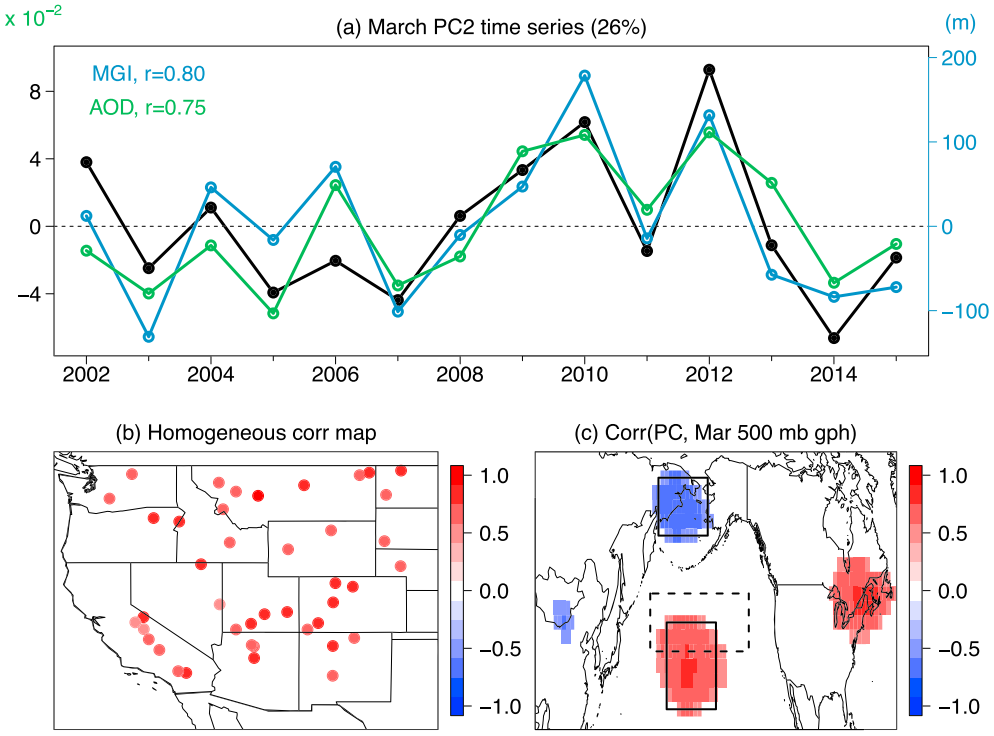

Figure 4. Analysis of the second EOF mode of standardized monthly anomalies of March fine dust concentrations between 2002 and 2015, which explains 26% of the total variance. (a) Time series of the principal components of the second EOF mode ("PC2," black). The panel also shows the detrended March time series of our custom index describing the meridional gradient of 500 mb geopotential heights across the North Pacific ("MGI," blue) and the detrended March time series of MODIS 550 nm aerosol optical depth (AOD, green). The MGI is calculated as the difference in the 500 mb geopotential heights between two domains over the North Pacific Ocean: 57.5°–67.5°N, 165°E–165°W and 27.5°–42.5°N, 170°E–160°W, outlined by the black boxes in Figure 4c. MODIS AOD is averaged over a domain in between these two pressure centers over the North Pacific Ocean (37.5°–47.5°N, 160°E–140°W), outlined by the dashed box in Figure 4c. Correlations of the two indices with March PC2 are shown inset. The left axis corresponds to PC2 values and AOD values scaled by 10^{-2}, and the right axis corresponds to MGI values (m). (b) Homogeneous correlation map between PC2 and the time series of standardized monthly fine dust anomalies at IMPROVE sites. (c) Heterogeneous correlation map between PC2 and March 500 mb geopotential height (gph). In Figures 4b and 4c, only those sites or grid cells with statistically significant correlations ($p < 0.05$) are shown. Monthly meteorological variables are detrended but not standardized.

Northwest is cooler and wetter from February to April. As in March PC1, modulation of the trans-Pacific transport path of Asian dust by ENSO is likely an additional contributing factor.

In May, we find that it is instead the pattern of coherent covariability across the western United States that is associated with ENSO and PDO. This first EOF mode accounts for 49% of the total variance (Figure S6). The associated principal component time series, PC1, is significantly correlated to several 3 month running mean climate indices during the previous-year late summer to current-year spring season. The highest correlations are found for current-year FMA ENSO ONI ($r = -0.63$) and previous-year September-November (SON) PDO ($r = -0.63$). By May, the Northwest-Southwest dipole pattern of precipitation and temperature anomalies driven by ENSO is replaced by an almost uniform pattern across the western United States (NOAA Climate Prediction Center). Positive PC1 years are associated with warmer and drier conditions across the West in May. Such widespread anomalies appear to be driven by a combination of two factors: (1) constructive interference between La Niña conditions and negative PDO conditions during the previous-year fall to current-year spring (e.g., Weiss et al., 2009) and (2) an anomalous blocking anticyclone in the midtroposphere over the west coast of the United States during May, as seen from 500 mb geopotential height anomalies (Figure S6c). This anomalous midtropospheric geopotential height pattern resembles the "Ridiculously Resilient Ridge," a persistent midtropospheric high-pressure system in the Northeast Pacific that deflected the Pacific storm track northward during the 2012–2015 cool season (October–May), contributing to drought conditions in California (Swain et al., 2014, 2016).

Table 1
A Summary of the Dominant Spatial Patterns of the Interannual Variability in Fine Dust Concentrations Between 2002 and 2015 March–May in the Western United States, and the Meteorological Controlling Factors, as Identified by EOF and Correlation Analyses

EOF mode	Spatial pattern of covariability	Percentage of total variance explained	Controlling factors
March EOF1	Northwest-Southwest dipole	28%	• Regional January–March precipitation, air temperature, relative humidity, and soil moisture driven by ENSO[a] and PDO[b] • Northward shift of trans-Pacific transport path of Asian dust during El Niño; southward shift during La Niña
March EOF2	Coherent across the West	26%	• Strength of trans-Pacific transport of Asian dust in March
April EOF1	Coherent across the West	33%	• Regional February-April precipitation • Strength of trans-Pacific transport of Asian dust in April
April EOF2	Northwest-Southwest dipole	21%	• February-April air temperature and soil moisture in Southwest regions, driven by ENSO[a] • Northward shift of trans-Pacific transport path of Asian dust during El Niño; southward shift during La Niña
May EOF1	Coherent across the West	49%	• Regional May precipitation, air temperature and relative humidity, driven by ENSO[a], PDO[b], and midlevel atmospheric circulation
May EOF2	Coherent across Arizona and New Mexico	12%	• Regional March-May precipitation • May soil moisture in New Mexico, Texas, and Mexico

[a]El Niño–Southern Oscillation. [b]Pacific Decadal Oscillation.

The remaining modes, April EOF1 and May EOF2, appear to be driven by a combination of factors. The first EOF mode for April, which explains 33% of the total variance, consists of a pattern of coherent covariability across the western United States (Figure S7). This EOF mode is associated with anomalies in average FMA precipitation across the West, though the correlations are not very spatially extensive. In positive PC1 years, precipitation is generally lower across the West and fine dust concentrations are higher. We also find significant correlations between April PC1 and 500 mb geopotential height anomalies over the Asian dust outflow region, suggesting a contribution of Asian dust in this EOF mode. Composite anomalies of 500 mb geopotential height and wind fields associated with positive PC1 years indicate that the coupling of a cyclonic circulation over the source region and an anticyclonic circulation over the Northwest Pacific Ocean enhances Asian dust convective outflow and trans-Pacific transport (Figures S7d and S7e). Our results are consistent with Creamean et al. (2014), who identified two main pathways of trans-Pacific transport of Asian dust during the spring months between 2002 and 2011: (1) meridional excursions north into Alaska and then south along the U.S. west coast and (2) zonal transport over the North Pacific Ocean. The composite wind field anomalies in Figure S7e suggest that pathway 1 applies to this EOF mode. Indeed, we find that the detrended April monthly mean time series of MODIS AOD averaged over a domain centered over the high-pressure center (45°–55°N, 160°–180°E, outlined in Figure S7d) is significantly correlated to PC1 ($r = 0.79$).

Finally, the second EOF mode for May features a pattern of covariability in Arizona and New Mexico and accounts for 12% of the total variance (Figure S8). We find that PC2 is correlated to a Northwest-Southwest dipole pattern of MAM precipitation anomalies and to May SPEI03 values spanning regions in New Mexico, Texas, and Mexico. Positive PC2 years, in which fine dust concentrations are higher, are associated with lower than average regional precipitation and soil moisture in neighboring regions to the southeast.

A summary of the dominant EOF modes and their controlling factors are described in Table 1. To corroborate the above EOF results obtained using $PM_{2.5}$-Iron as a fine dust proxy, we repeated the analysis with $PM_{2.5}$-Calcium. The resulting dominant spatial patterns of covariability are similar to those using $PM_{2.5}$-Iron (section S4 and Figure S9).

3.3. Controlling Factors of the 2002–2015 Increase in March Fine Dust Concentrations in the Southwest

Most IMPROVE sites located south of 40°N display increasing trends in March fine dust concentrations between 2002 and 2015, with statistically significant trends for 19 out of the 42 sites located between 33°–39.5°N and 103°–121°W (regional average of 0.06 ± 0.04 μg m^{-3} a^{-1}). In this section, we investigate

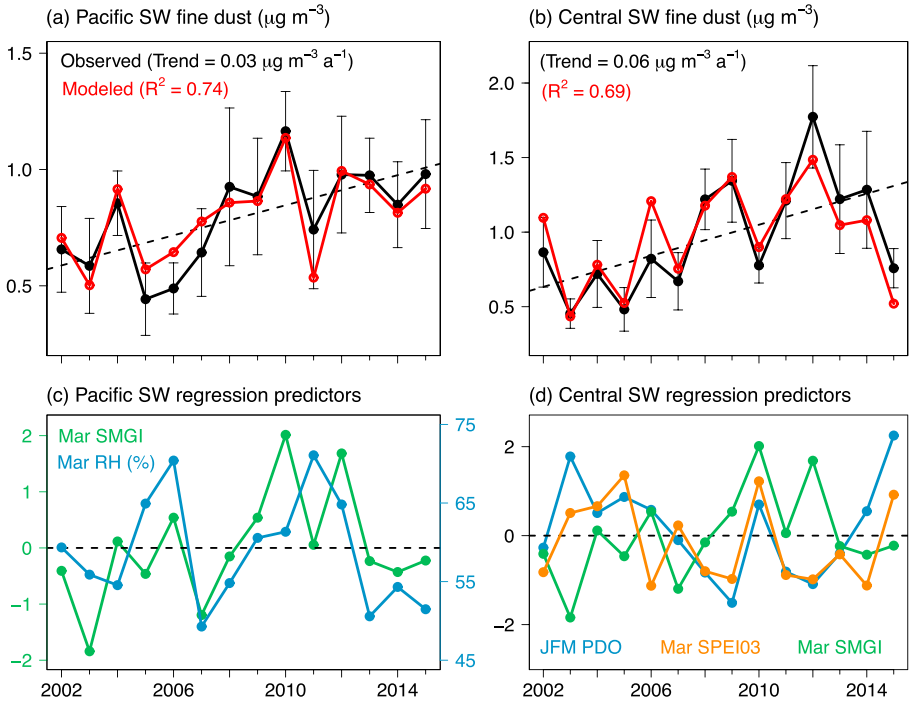

Figure 5. (a) The 2002–2015 time series of observed (black) and modeled (red) March monthly mean fine dust concentrations averaged over sites in the Pacific Southwest domain (33°–39.5°N, 115.5°–121°W; see Figure 1). Error bars denote one standard deviation of the observed means. The black dotted line denotes the linear trend of observed regional fine dust between 2002 and 2015. Predicted values are calculated using a multiple linear regression model with meteorological variables and standard climate indices as predictors. The adjusted coefficient of multiple determination, R^2, of the model is shown inset. (b) As in Figure 5a but for the Central Southwest domain (33°–39.5°N, 103°–115°W). (c) The 2002–2015 time series of the two variables selected by the regression method for the Pacific Southwest domain: March Standardized Meridional Gradient Index (SMGI, green) of the 500 mb geopotential heights; and March regional relative humidity (RH, blue). The left axis corresponds to SMGI values (unitless) and the right axis corresponds to RH values (%). (d) The 2002–2015 time series of the three variables selected by the regression method for the Central Southwest domain (all unitless): JFM Pacific Decadal Oscillation (PDO, blue); March 3-month Standardized Precipitation-Evapotranspiration Index (SPEI03, orange); and March Standardized Meridional Gradient Index (SMGI, green) of the 500 mb geopotential heights.

potential causes of this increase. As Figure 1 (bottom) shows, out of the 19 sites displaying statistically significant increases in this region, 17 are located at elevations greater than 1,000 m above sea level (asl). In general, high-elevation sites have smaller monthly mean fine dust concentrations and standard deviations averaged over the 14 year period relative to those at or below 1,000 m asl. It is likely that the low-elevation sites experience greater variability and concentrations due to their proximity to two large sources of natural dust, the Mojave and Sonoran Deserts, and/or to urban centers. Hand et al. (2012) found that 2005–2008 monthly mean fine dust concentrations in the Southwest were highest at sites located in rural southern Arizona and in urban areas. In a more recent study, Hand et al. (2017) found that 2011–2014 coarse mass PM concentrations were inversely correlated with elevation at IMPROVE sites located in the western United States.

Our March EOF analysis (section 3.2) suggests that fine dust concentrations in California are partially controlled by factors different from those in Arizona, New Mexico, Colorado, and Utah. We therefore divide this region into two domains: "Pacific Southwest" (33°–39.5°N, 115.5°–121°W) and "Central Southwest" (33°–39.5°N, 103°–115°W), as outlined in Figure 1. The 2002–2015 time series of regional mean March fine dust concentrations reveal statistically significant linear trends of +0.03 μg m^{-3} a^{-1} for the Pacific Southwest domain (Figure 5a), and +0.06 μg m^{-3} a^{-1} for the Central Southwest domain (Figure 5b). For the Central Southwest regional mean calculation, we exclude measurements from the colocated Phoenix sites ("PHOE1" and "PHOE5"), as these urban sites appear to be an outlier in both the observed trend and average fine dust concentrations measured between 2002 and 2015.

For each of the two time series, we construct a multiple linear regression model from a set of potential predictors, following the stepwise approach described in section 2.5. Results from the EOF analysis in section 3.2 guided our choice of predictors. These include (1) JFM ENSO ONI; (2) JFM PDO; (3) March standardized meridional gradient index (SMGI) of 500 mb geopotential heights, calculated as the difference between the 500 mb geopotential heights averaged over two domains: 27.5°–42.5°N, 170°E–160°W and 57.5°–67.5°N, 165°E–165°W, and subsequently standardized; (4) regional March and JFM precipitation; (5) regional March and JFM surface relative humidity; and (6) regional March SPEI03 values. Variables 4–6 are averaged over the same domain as fine dust except for SPEI03 for the Central Southwest domain, for which values are averaged over a domain spanning Arizona, New Mexico, and northern Mexico (26°–35°N, 115°–103°W) in which the correlations between March PC1 and SPEI03 are most extensive.

For the Pacific Southwest, the resulting model is of the form:

$$[\text{Fine dust}] = 0.20 \times \text{SMGI} - 0.02 \times \text{RH} + 2.11, \quad (1)$$

where "Fine dust" refers to the March monthly mean fine dust concentrations ($\mu g\ m^{-3}$) averaged over all sites in the Pacific Southwest domain, SMGI is our custom standardized index to represent the March meridional gradient in 500 mb geopotential heights over the Northern Pacific Ocean, and RH is the March regional relative humidity. This regression fit, shown in Figure 5a, captures 74% of the variance in the 2002–2015 March time series of regional fine dust, with a modeled trend of 0.03 ($\mu g\ m^{-3}\ a^{-1}$). We also assess the predictive power of the chosen model by applying "leave-one-out" cross validation, which estimates regression coefficients based on all the data except for one point and makes a prediction for that point each round. The squared correlation coefficient between the observed values and predicted values from this process is 0.59, suggesting that the model is not overfitted.

We interpret the conditions driving the variability and trend in March fine dust in the Pacific Southwest as follows. First, the 2002–2015 interannual variability of fine dust concentrations, though not the long-term trend, appears to be influenced by regional relative humidity. Laboratory and field studies have demonstrated that for relative humidity greater than 40%, increases in relative humidity enhance soil particle cohesion, reducing mobilization (Csavina et al., 2014; Neuman & Sanderson, 2008). As Figure 5c shows, surface relative humidity averaged over the Pacific Southwest domain in March is above 45%. Second, the 2002–2015 trend in regional fine dust concentrations appears to be associated with variations in Asian dust transport. In the early part of the time period, from 2002 to 2010, the March meridional gradient in 500 mb geopotential heights over the North Pacific Ocean increased slightly (linear trend in SMGI = 0.25 a^{-1}, $p = 0.1$), resulting in stronger westerly winds and most likely trans-Pacific transport of Asian dust to the western United States. Our results are consistent with Creamean et al. (2014), who demonstrated that from 2002 to 2011, Asian dust contributed more than local sources to dust measured at high-elevation IMPROVE sites in California during the spring months. Comparing the changes in the coefficient of multiple determination (R^2) when each variable is added to the model last reveals that SMGI is the primary controlling factor of the observed fine dust variability.

For the Central Southwest, the resulting model is of the form

$$[\text{Fine dust}] = -0.09 \times \text{PDO} - 0.21 \times \text{SPEI03} + 0.13 \times \text{SMGI} + 0.95, \quad (2)$$

where "Fine dust" refers to the March monthly mean fine dust concentrations ($\mu g\ m^{-3}$) averaged over all sites in the Central Southwest domain, PDO is the JFM Pacific Decadal Oscillation Index values, SPEI03 is the March 3-month Standardized Precipitation-Evapotranspiration Index averaged over a domain spanning Arizona, New Mexico, and northern Mexico, and SMGI is our custom standardized index to represent the March 500 mb geopotential height meridional gradient over the Northern Pacific Ocean. This regression fit, shown in Figure 5b, captures 69% of the variance in the 2002–2015 March time series of regional fine dust, with a modeled trend of 0.05 $\mu g\ m^{-}3\ a^{-1}$ ($p = 0.38$). The squared correlation coefficient between the observed values and predicted values from leave-one-out cross validation is 0.48.

We interpret the conditions resulting in the March fine dust trend in the Central Southwest as follows. First, for 5 of the 8 years since 2007, both ENSO and PDO were in the negative phase during JFM, (Figures 3a and 5d), resulting in drier and warmer conditions across the Southwest. Second, as Figure 5d shows, the March SPEI03 averaged over Arizona, New Mexico, and northern Mexico generally decreased between 2005 and 2015, with

abrupt increases in 2010 and 2015. The 2010 and 2015 increases represent the response to relatively strong El Niño and positive PDO events in the preceding winter. Because this domain encompasses parts of the Mojave, Sonoran, and Chihuahuan Deserts, it is most likely that reduced soil moisture led to greater dust emissions from these sources. The percentage area of lands experiencing "abnormally dry," "moderate drought," or "severe drought" conditions averaged over Arizona and New Mexico showed large but variable increases over the 2000–2015 time frame in January to March (Figure S10). Third, as described above, the March meridional gradient in 500 mb geopotential heights over the North Pacific Ocean increased slightly between 2002 and 2010. Comparing the changes in the coefficient of multiple determination when each variable is added to the model reveals that SPEI03 is the most important controlling factor, followed by SMGI. We attribute the apparent weakening of the positive dust trend in the most recent years (2013–2015) to the PDO switching from negative to positive phase, in conjunction with neutral ENSO conditions during January–March. These two phenomena resulted in relatively cool and wet conditions in the Southwest.

None of the explanatory variables chosen in the regression fits for both domains display statistically significant linear trends over the entire 2002–2015 time period. However, with only 14 years of observations available, it is difficult to discern whether the observed dust trends are mainly due to natural variability of these drivers or whether significant long-term changes of the drivers have yet to emerge. Using the above regression fits to predict each domain's regional mean fine dust concentrations between 1990 and 2001, we do not find significant trends in fine dust concentrations or predictor values between 1990 and 2001 (Figures S11 and S12).

4. Discussion and Conclusions

In this study, we perform a systematic statistical analysis to identify the dominant spatial patterns of fine dust interannual variability between 2002 and 2015 March–May across the western United States, and their meteorological controlling factors. Using empirical orthogonal function (EOF) analysis, we find that 54–61% of the fine dust interannual variability in each spring month is captured by the first two leading modes, which consist of a pattern of coherent covariability across the western United States and a Northwest-Southwest dipole of variability. These broad-scale patterns of fine dust interannual variability are mainly associated with regional precipitation, surface temperature, and soil moisture anomalies. The strength of the trans-Pacific transport and outflow of Asian dust also likely contributes to fine dust variability in March and April. These controlling factors in turn tend to be driven by large-scale sea surface temperature and/or atmospheric circulation anomalies. In particular, El Niño–Southern Oscillation in winter-to-early spring appears to play a large role in modulating fine dust variability in all spring months. Our results are consistent with previous studies suggesting that in addition to local influences, fine dust levels across the western United States are also associated with large-scale controlling mechanisms and Asian dust contributions (e.g., Creamean et al., 2014; Kavouras et al., 2009; Malm et al., 2004).

We find that the March monthly mean fine dust concentrations have significantly increased by 0.03 $\mu g\ m^{-3}\ a^{-1}$ from 2002 to 2015 averaged over sites in the Pacific Southwest and by 0.06 $\mu g\ m^{-3}\ a^{-1}$ for sites in the Central Southwest. Using multiple linear regression analysis, we find that 74% of the variance in the observed 2002–2015 time series of fine dust averaged over the Pacific Southwest domain can be explained by two predictors: (1) strength of the trans-Pacific transport of Asian dust during March and (2) regional monthly mean relative humidity. For the Central Southwest fine dust time series, 69% of the variance can be explained by three factors: (1) regional JFM precipitation and temperature anomalies influenced by the wintertime Pacific Decadal Oscillation and El Niño–Southern Oscillation, (2) soil moisture conditions averaged over Arizona, New Mexico, and northern Mexico represented by the March 3-month Standardized Precipitation-Evapotranspiration Index, and (3) strength of the trans-Pacific transport of Asian dust during March. None of these factors exhibit significant long-term trends between 2002 and 2015, but their combination can partially explain the observed, significant dust increases.

Our results demonstrate that springtime fine dust activity in the U.S. Southwest is strongly linked to regional hydroclimate variability in the preceding winter and concurrent spring (January–May). This includes soil moisture fluctuations in the Mojave, Sonoran, and Chihuahuan Desert regions of North America, which are important sources of natural dust for the Southwest (Jewell & Nicoll, 2011; Reynolds et al., 2007; Rivera Rivera et al., 2010). Many studies have emphasized the role of antecedent precipitation in regulating dust

activity through controlling wet deposition of atmospheric dust, soil moisture, and vegetation cover (e.g., Elmore et al., 2008; Zender & Kwon, 2005), including local-scale studies in the Southwest (e.g., Bach & Brazel, 1996; Reheis & Urban, 2011; Urban et al., 2009). Laboratory and field studies have also demonstrated that increases in relative humidity can reduce dust emissions by increasing soil particle cohesion (Csavina et al., 2014; Neuman & Sanderson, 2008).

Consistent with Okin and Reheis (2002) and Hand et al. (2016), we find that when ENSO and PDO are both in the negative phase during the winter to early spring, the Southwest tends to experience drought conditions and elevated springtime fine dust levels. In fact, we find that the correlation coefficient of the 2002–2015 time series of JFM ENSO ONI and PDO indices is 0.69, compared to 0.44 between 1981 and 2011. This result suggests that during the 14 year period of our study, constructive interference between ENSO and PDO may have amplified the regional hydroclimate impacts of these two phenomena. Other studies, however, have shown that periods of extreme wetness, including those driven by extreme El Niño events, can also be followed by enhanced dust activity in the Southwest, most likely due to the supply of flood sediments (Okin & Reheis, 2002; Zender & Kwon, 2005). We do not find evidence of this effect here.

Our results suggest that Asian dust exerts an influence over fine dust concentrations across the western U.S. through variations in the strength of the midtroposphere westerly flow over the central North Pacific Ocean and of the dust outflow from the Asian continent. This contribution is distinguishable in March and April, but not in May, at least for the 2002–2015 time period. Consistent with our results, Fischer et al. (2009) found that ~80% of the 1998–2007 interannual variability of springtime mean $PM_{2.5}$ in the northwest U.S. can be explained by indices that represent the variability in Asian dust emissions and transport and by regional precipitation. In a model study, Zhao et al. (2006) simulated a 44 year (1960–2003) climatology of Asian dust trans-Pacific transport and found that springtime inflow of Asian dust to the North American continent is greatest in April, followed by May, then March. Reasons for the discrepancy between Zhao et al. (2006) and our results are not clear but may be linked to the observed 1.1 m s^{-1} a^{-1} increase ($p = 0.16$) in 500 mbar zonal wind speeds over the central North Pacific Ocean in March over 2003–2013, nearly concurrent with a 1.2 m s^{-1} a^{-1} decrease ($p < 0.01$) in these winds in May over 2002–2010.

Hand et al. (2016) proposed that the observed increase in March fine dust concentrations across the Southwest from 1995 to 2014 is due to an earlier onset of the spring dust season and a shift of the PDO to the negative phase, resulting in drier, windier, and less vegetated conditions. Our study extends Hand et al. (2016) by systematically analyzing the meteorological controlling factors of fine dust on interannual time scales and by developing a prediction model for the observed March fine dust time series. Consistent with Hand et al. (2016), we find that the JFM PDO index is a good predictor of the 2002–2015 fine dust time series for the Southwest domain. In addition, we find that soil moisture reductions in a domain spanning the Mojave, Sonoran, and Chihuahuan Deserts, and increases in the strength of the trans-Pacific transport of Asian dust may have also contributed to the observed trend. Our results suggest that this trend in March fine dust is linked to natural variability of multiple drivers, though significant long-term changes of one or more drivers may have yet to emerge.

Several factors introduce uncertainty into our study. First, we used $PM_{2.5}$-Iron as a fine dust proxy and assumed average crustal abundances across the IMPROVE network. However, there are other sources of atmospheric iron besides mineral sources, and the mineral composition can vary for different types of soils. We are also limited in terms of temporal coverage. The IMPROVE network has robust spatial coverage across the western United States only from 2002 onward. Although surface wind speed is a well-established driving factor of dust generation on local scales (e.g., Csavina et al., 2014; Kok et al., 2012), we do not find significant correlations between this variable and fine dust on interannual time scales. This lack of correlation is likely due in part to our focus on monthly mean quantities and in part to the limitations of reanalysis data, which cannot resolve local complex terrain and wind dynamics, even at the finest spatial scales (Huang et al., 2015; Jewell & Nicoll, 2011). There are also other potentially important controlling factors of dust generation not considered in this study, such as vegetation dynamics, surface bareness, and human land use. Lark (2015) recently found that the Southern Great Plains experienced extensive cropland expansion between 2008 and 2012, which could be a contributing factor to the observed increase in Southwest fine dust concentrations. However, it is not clear why this anthropogenic source would have the greatest impact in March only.

To our knowledge, our study is the first to diagnose the dominant spatial patterns of springtime fine dust interannual variability across the western United States and their meteorological controlling factors. Better understanding of the observed relationships between dust and meteorological variables will allow us to improve dust modeling skills, as well as provide an observational foundation for estimating future dust activity under a range of climate change scenarios that is not restricted by the ability of a given model to capture dust mobilization and lifetimes. Moreover, our statistical models for predicting March fine dust concentrations in the Southwest enabled us to identify the primary mechanisms underlying the observed increases over the past decade.

Without aggressive reductions in global greenhouse gas emissions, the U.S. Southwest is projected to experience unprecedented drought conditions within this century (e.g., Ault et al., 2016; Cook et al., 2015; Seager & Vecchi, 2010). Future changes in ENSO and PDO in response to climate change remain inconclusive (Cai et al., 2015; Wang et al., 2014), though results from a multimodel ensemble study by Kwon et al. (2013) suggest that the linear relationship between ENSO and PDO during the boreal winter (December–February) may become stronger under greenhouse gas forcing. Asian dust outflow to the Pacific appears to have increased as a result of desertification (Chin et al., 2003), but it is not known if and how climate change will influence trans-Pacific transport in the future. Land disturbance from human activities may enhance desertification in northern China as well as the U.S. Southwest and Great Plains (Brahney et al., 2013; Feng et al., 2015). With the Southwest population projected to reach ~75 million by 2030, an increase of 34% relative to 2010 (Theobald et al., 2013), the likelihood of higher dust levels poses air quality and public health threats to the region.

Acknowledgments
This research was developed under Assistance Agreement 83587501 awarded by the U.S. Environmental Protection Agency (EPA). It has not been formally reviewed by the EPA. The views expressed in this document are solely those of the authors and do not necessarily reflect those of the EPA. The EPA does not endorse any products mentioned in this publication. The authors thank Xu Yue (Institute of Atmospheric Physics, Chinese Academy of Sciences) for helpful discussions, and Richard L. Reynolds and two anonymous reviewers for constructive comments. We also thank all of the data providers of the data sets used in this study. Aerosol data were provided by the Interagency Monitoring of Protected Visual Environments (IMPROVE; available online at http://vista.cira.colostate.edu/improve). IMPROVE is a collaborative association of state, tribal, and federal agencies, and international partners. U.S. Environmental Protection Agency is the primary funding source, with contracting and research support from the National Park Service. The Air Quality Group at the University of California, Davis, is the central analytical laboratory, with ion analysis provided by Research Triangle Institute, and carbon analysis provided by Desert Research Institute. Meteorological data and standard climate indices were provided by the Oregon State University PRISM Climate Group (http://prism.oregonstate.edu/), NOAA/OAR/ESRL PSD (http://www.esrl.noaa.gov/psd/), NOAA Climate Prediction Center (http://www.cpc.noaa.gov/), and the NASA Goddard Earth Sciences Data and Information Services Center (GES DISC; https://disc.gsfc.nasa.gov/). The Standardized Precipitation-Evapotranspiration Index was provided by the Spanish National Research Council (http://spei.csic.es/database.html). The MODIS Dark Target 550 nm AOD products were processed using the GES-DISC Interactive Online Visualization and Analysis Infrastructure (Giovanni; https://giovanni.sci.gsfc.nasa.gov/). Data analysis was conducted using the open source R and the NCAR Command Language (NCL) programming languages.

References

Alvera-Azcárate, A., Barth, A., Rixen, M., & Beckers, J. (2005). Reconstruction of incomplete oceanographic data sets using empirical orthogonal functions: Application to the Adriatic Sea surface temperature. *Ocean Modelling*, *9*(4), 325–346. https://doi.org/10.1016/j.ocemod.2004.08.001

Ault, T. R., Mankin, J., Cook, B. I., & Smerdon, J. E. (2016). Relative impacts of mitigation, temperature, and precipitation on 21st-century megadrought risk in the American Southwest. *Science Advances*, *2*(10), e1600873. https://doi.org/10.1126/sciadv.1600873

Bach, A., & Brazel, A. (1996). Temporal and spatial aspects of blowing dust in the Mojave and Colorado deserts of southern California, 1973–1994. *Physical Geography*, *17*(4), 329–353. https://doi.org/10.1080/02723646.1996.10642589

Beckers, J. M., & Rixen, M. (2003). EOF calculations and data filling from incomplete oceanographic datasets. *American Meteorological Society*, *20*, 1839–1856.

Brahney, J., Ballantyne, A. P., Sievers, C., & Neff, J. C. (2013). Increasing Ca2+ deposition in the western US: The role of mineral aerosols. *Aeolian Research*, *10*, 77–87. https://doi.org/10.1016/j.aeolia.2013.04.003

Cai, W., Santoso, A., Wang, G., Yeh, S.-W., An, S.-I., Cobb, K. M., … Wu, L. (2015). ENSO and greenhouse warming. *Nature Publishing Group*, *5*(9), 849–859. https://doi.org/10.1038/nclimate2743

Carmona, J. M., Vanoye, A. Y., Lozano, F., & Mendoza, A. (2015). Dust emission modeling for the western border region of Mexico and the USA. *Environment and Earth Science*, *74*(2), 1687–1697. https://doi.org/10.1007/s12665-015-4173-5

Carslaw, K. S., Boucher, O., Spracklen, D. V., Mann, G. W., Rae, J. G. L., Woodward, S., & Kulmala, M. (2010). Atmospheric aerosols in the Earth system: A review of interactions and feedbacks. *Atmospheric Chemistry and Physics*, *10*(4), 1701–1737. https://doi.org/10.5194/acp-10-1701-2010

Chin, M., Ginoux, P., Lucchesi, R., Huebert, B., Weber, R., Anderson, T., … Thornton, D. (2003). A global aerosol model forecast for the ACE-Asia field experiment. *Journal of Geophysical Research*, *108*(D23), 8654. https://doi.org/10.1029/2003JD003642

Cook, B. I., Ault, T. R., & Smerdon, J. E. (2015). Unprecedented 21st century drought risk in the American Southwest and Central Plains. *Science Advances*, *1*(1), e1400082. https://doi.org/10.1126/sciadv.1400082

Creamean, J. M., Spackman, J. R., Davis, S. M., White, A. B., Spackman, J. R., Davis, S. M., & White, A. B. (2014). Climatology of long-range transported Asian dust along the West Coast of the United States. *Journal of Geophysical Research: Atmospheres*, *119*, 12,171–12,185. https://doi.org/10.1002/2014JD021694

Crooks, J. L., Cascio, W. E., Percy, M. S., Reyes, J., Neas, L. M., & Hilborn, E. D. (2016). The association between dust storms and daily non-accidental mortality in the United States, 1993–2005. *Environmental Health Perspectives*, *124*(11), 1735–1743. https://doi.org/10.1289/EHP216

Csavina, J., Field, J., Félix, O., Corral-Avitia, A. Y., Sáez, A. E., & Betterton, E. A. (2014). Effect of wind speed and relative humidity on atmospheric dust concentrations in semi-arid climates. *Science of the Total Environment*, *487*(1), 82–90. https://doi.org/10.1016/j.scitotenv.2014.03.138

Csavina, J., Field, J., Taylor, M. P., Gao, S., Landázuri, A., Betterton, E. A., & Sáez, A. E. (2012). A review on the importance of metals and metalloids in atmospheric dust and aerosol from mining operations. *Science of the Total Environment*, *433*, 58–73. https://doi.org/10.1016/j.scitotenv.2012.06.013

Elmore, A. J., Kaste, J. M., Okin, G. S., & Fantle, M. S. (2008). Groundwater influences on atmospheric dust generation in deserts. *Journal of Arid Environments*, *72*(10), 1753–1765. https://doi.org/10.1016/j.jaridenv.2008.05.008

Fairlie, T. D., Jacob, D. J., & Park, R. J. (2007). The impact of transpacific transport of mineral dust in the United States. *Atmospheric Environment*, *41*(6), 1251–1266. https://doi.org/10.1016/j.atmosenv.2006.09.048

Feng, Q., Ma, H., Jiang, X., Wang, X., & Cao, S. (2015). What has caused desertification in China? *Scientific Reports*, *5*(1), 15998. https://doi.org/10.1038/srep15998

Fischer, E. V., Hsu, N. C., Jaffe, D. A., Jeong, M. J., & Gong, S. L. (2009). A decade of dust: Asian dust and springtime aerosol load in the U.S. Pacific Northwest. *Geophysical Research Letters*, *36*, L03821. https://doi.org/10.1029/2008GL036467

Flagg, C. B., Neff, J. C., Reynolds, R. L., & Belnap, J. (2014). Spatial and temporal patterns of dust emissions (2004–2012) in semi-arid landscapes, southeastern Utah, USA. *Aeolian Research*, *15*, 31–43. https://doi.org/10.1016/j.aeolia.2013.10.002

Gelaro, R., McCarty, W., Suárez, M. J., Todling, R., Molod, A., Takacs, L., … Zhao, B. (2017). The Modern-Era Retrospective Analysis For Research And Applications, version 2 (MERRA-2). *Journal of Climate*, *30*(14), 5419–5454. https://doi.org/10.1175/JCLI-D-16-0758.1

Gong, S. L., Zhang, X. Y., Zhao, T. L., Zhang, X. B., Barrie, L. A., McKendry, I. G., & Zhao, C. S. (2006). A simulated climatology of Asian dust aerosol and its trans-Pacific transport. Part II: Interannual variability and climate connections. *American Meteorological Society*, *19*(1), 104–122. https://doi.org/10.1175/JCLI3606.1

Goudie, A. S. (2014). Desert dust and human health disorders. *Environment International*, *63*, 101–113. https://doi.org/10.1016/j.envint.2013.10.011

Guirguis, K. J., & Avissar, R. (2008). A precipitation climatology and dataset intercomparison for the western United States. *Journal of Hydrometeorology*, *9*(5), 825–841. https://doi.org/10.1175/2008JHM832.1

Hahnenberger, M., & Nicoll, K. (2012). Meteorological characteristics of dust storm events in the eastern Great Basin of Utah, U.S.A. *Atmospheric Environment*, *60*, 601–612. https://doi.org/10.1016/j.atmosenv.2012.06.029

Hand, J. L., Gill, T. E., & Schichtel, B. A. (2017). Spatial and seasonal variability in fine mineral dust and coarse aerosol mass at remote sites across the United States. *Journal of Geophysical Research: Atmospheres*, *122*, 3080–3097. https://doi.org/10.1002/2016JD026290

Hand, J. L., Schichtel, B. A., Pitchford, M., Malm, W. C., & Frank, N. H. (2012). Seasonal composition of remote and urban fine particulate matter in the United States. *Journal of Geophysical Research*, *117*, D05209. https://doi.org/10.1029/2011JD017122

Hand, J. L., White, W. H., Gebhart, K. A., Hyslop, N. P., Gill, T. E., & Schichtel, B. A. (2016). Earlier onset of the spring fine dust season in the southwestern United States. *Geophysical Research Letters*, *43*, 4001–4009. https://doi.org/10.1002/2016GL068519

Herold, N., Kala, J., & Alexander, L. V. (2016). The influence of soil moisture deficits on Australian heatwaves. *Environmental Research Letters*, *11*(6), 1–8. https://doi.org/10.1088/1748-9326/11/6/064003

Huang, H.-Y., Capps, S. B., Huang, S.-C., & Hall, A. (2015). Downscaling near-surface wind over complex terrain using a physically-based statistical modeling approach. *Climate Dynamics*, *44*(1-2), 529–542. https://doi.org/10.1007/s00382-014-2137-1

Huneeus, N., Schulz, M., Balkanski, Y., Griesfeller, J., Prospero, J., Kinne, S., … Zender, C. S. (2011). Global dust model intercomparison in AeroCom phase I. *Atmospheric Chemistry and Physics*, *11*(15), 7781–7816. https://doi.org/10.5194/acp-11-7781-2011

Hyslop, N. P., Trzepla, K., & White, W. H. (2015). Assessing the Suitability of historical PM2.5 element measurements for trend analysis. *Environmental Science & Technology*, *49*(15), 9247–9255. https://doi.org/10.1021/acs.est.5b01572

Idso, S. B., Ingram, R. S., & Pritchard, J. M. (1972). An American haboob. *Bulletin of the American Meteorological Society*, *53*(10), 930–935. https://doi.org/10.1175/1520-0477(1972)053%3C0930:AAH%3E2.0.CO;2

Jewell, P. W., & Nicoll, K. (2011). Wind regimes and aeolian transport in the Great Basin, U.S.A. *Geomorphology*, *129*(1-2), 1–13. https://doi.org/10.1016/j.geomorph.2011.01.005

Jickells, T. D. (2005). Global iron connections between desert dust, ocean biogeochemistry, and climate. *Science*, *308*(5718), 67–71. https://doi.org/10.1126/science.1105959

Kanamitsu, M., Ebisuzaki, W., Woollen, J., Yang, S. K., Hnilo, J. J., Fiorino, M., & Potter, G. L. (2002). NCEP-DOE AMIP-II reanalysis (R-2). *Bulletin of the American Meteorological Society*, *83*(11), 1631–1643. https://doi.org/10.1175/BAMS-83-11-1631

Kavouras, I. G., Etyemezian, V., DuBois, D. W., Xu, J., & Pitchford, M. (2009). Source reconciliation of atmospheric dust causing visibility impairment in Class I areas of the western United States. *Journal of Geophysical Research*, *114*, D02308. https://doi.org/10.1029/2008JD009923

Kavouras, I. G., Etyemezian, V., Xu, J., DuBois, D. W., Green, M., & Pitchford, M. (2007). Assessment of the local windblown component of dust in the western United States. *Journal of Geophysical Research*, *112*, D08211. https://doi.org/10.1029/2006JD007832

Kim, K.-H., Kabir, E., & Kabir, S. (2015). A review on the human health impact of airborne particulate matter. *Environment International*, *74*, 136–143. https://doi.org/10.1016/j.envint.2014.10.005

Kok, J. F., Parteli, E. J. R., Michaels, T. I., & Karam, D. B. (2012). The physics of wind-blown sand and dust. *Reports on Progress in Physics*, *75*(10), 106,901. https://doi.org/10.1088/0034-4885/75/10/106901

Kutner, M. H., Nachtscheim, C. J., Neter, J., & Li, W. (2004). *Applied linear statistical models*. New York, NY: McGraw-Hill/Irwin.

Kwon, M., Yeh, S. W., Park, Y. G., & Lee, Y. K. (2013). Changes in the linear relationship of ENSO-PDO under the global warming. *International Journal of Climatology*, *33*(5), 1121–1128. https://doi.org/10.1002/joc.3497

Lark, T. J., Meghan Salmon, J., & Gibbs, H. K. (2015). Cropland expansion outpaces agricultural and biofuel policies in the United States. *Environmental Research Letters*, *10*(4), 044003. https://doi.org/10.1088/1748-9326/10/4/044003

Lawrence, C. R., & Neff, J. C. (2009). The contemporary physical and chemical flux of aeolian dust: A synthesis of direct measurements of dust deposition. *Chemical Geology*, *267*(1–2), 46–63. https://doi.org/10.1016/j.chemgeo.2009.02.005

Lei, H., & Wang, J. X. L. (2014). Observed characteristics of dust storm events over the western United States using meteorological, satellite, and air quality measurements. *Atmospheric Chemistry and Physics*, *14*(15), 7847–7857. https://doi.org/10.5194/acp-14-7847-2014

Malm, W. (1999). *Introduction to visibility*, National Park Service and Colorodo State Institute for Research on the Atmosphere for Research on the Atmosphere, Colorodo State Institute, Fort Collins, CO.

Malm, W. C., Pitchford, M. L., McDade, C., & Ashbaugh, L. L. (2007). Coarse particle speciation at selected locations in the rural continental United States. *Atmospheric Environment*, *41*(10), 2225–2239. https://doi.org/10.1016/j.atmosenv.2006.10.077

Malm, W. C., Schichtel, B. A., Pitchford, M. L., Ashbaugh, L. L., & Eldred, R. A. (2004). Spatial and monthly trends in speciated fine particle concentration in the United States. *Journal of Geophysical Research*, *109*, D03306. https://doi.org/10.1029/2003JD003739

Malm, W. C., Sisler, J. F., Huffman, D., Eldred, R. A., & Cahill, T. A. (1994). Spatial and seasonal trends in particle concentration and optical extinction in the United States. *Journal of Geophysical Research*, *99*(D1), 1347–1370. https://doi.org/10.1029/93JD02916

Mansell, G., Lester, J., & Pollack, A. (2007). Studies of emissions from anthropogenic and natural dust sources in the western United States. *Journal of the Air & Waste Management Association*, 23–26.

Mantua, N. J., Hare, S. R., Zhang, Y., Wallace, J. M., & Francis, R. C. (1997). A Pacific interdecadal climate oscillation with impacts on salmon production. *Bulletin of the American Meteorological Society*, *78*(6), 1069–1079. https://doi.org/10.1175/1520-0477(1997)078%3C1069:APICOW%3E2.0.CO;2

McLennan, S. M. (2001). Relationships between the trace element composition of sedimentary rocks and upper continental crust. *Geochemistry, Geophysics, Geosystems*, *2*(4), 1021. https://doi.org/10.1029/2000GC000109

Middleton, N. J. (2017). Desert dust hazards: A global review. *Aeolian Research*, *24*, 53–63. https://doi.org/10.1016/j.aeolia.2016.12.001

Miller, R. L., Knippertz, P., Garcia-Pando, C. P., Perlwitz, J. P., & Tegen, I. (2014). Chapter 13: Impact of dust radiative forcing upon climate. In *Mineral dust: A key player in the Earth system* (pp. 1–509). Netherlands: Springer.

Mock, C. J. (1996). Climatic controls and spatial variations of precipitation in the western United States. *Journal of Climate*, *9*(5), 1111–1125. https://doi.org/10.1175/1520-0442(1996)009%3C1111:CCASVO%3E2.0.CO;2

Nam, J., Wang, Y., Luo, C., & Chu, D. A. (2010). Trans-Pacific transport of Asian dust and CO: accumulation of biomass burning CO in the subtropics and dipole structure of transport. *Atmospheric Chemistry and Physics*, *10*(7), 3297–3308. https://doi.org/10.5194/acp-10-3297-2010

Neff, J. C., Ballantyne, A. P., Farmer, G. L., Mahowald, N. M., Conroy, J. L., Landry, C. C., … Reynolds, R. L. (2008). Increasing eolian dust deposition in the western United States linked to human activity. *Nature Geoscience*, *1*(3), 189–195. https://doi.org/10.1038/ngeo133

Neuman, C. M., & Sanderson, S. (2008). Humidity control of particle emissions in aeolian systems. *Journal of Geophysical Research*, *113*, F02S14. https://doi.org/10.1029/2007JF000780

Okin, G. S., & Reheis, M. C. (2002). An ENSO predictor of dust emission in the southwestern United States. *Geophysical Research Letters*, *29*(9), 1332 . https://doi.org/10.1029/2001GL014494

Painter, T. H., Barrett, A. P., Landry, C. C., Neff, J. C., Cassidy, M. P., Lawrence, C. R., … Farmer, G. L. (2007). Impact of disturbed desert soils on duration of mountain snow cover. *Geophysical Research Letters*, *34*, L12502. https://doi.org/10.1029/2007GL030284

Painter, T. H., Deems, J. S., Belnap, J., Hamlet, A. F., Landry, C. C., & Udall, B. (2010). Response of Colorado River runoff to dust radiative forcing in snow. *Proceedings of the National Academy of Sciences of the United States of America*, *107*(40), 17,125–17,130. https://doi.org/10.1073/pnas.0913139107

Plumlee, G. S., & Ziegler, T. L. (2007). The medical geochemistry of dusts, soils, and other Earth materials. In H. D. Holland & K. K. Turekian (Eds.), *Treatise on geochemistry* (pp. 1–61). Oxford: Pergamon. https://doi.org/10.1016/B0-08-043751-6/09050-2

Raman, A., Arellano, A. F., & Brost, J. J. (2014). Revisiting haboobs in the southwestern United States: An observational case study of the 5 July 2011 Phoenix dust storm. *Atmospheric Environment*, *89*, 179–188. https://doi.org/10.1016/j.atmosenv.2014.02.026

Reheis, M. C., & Urban, F. E. (2011). Regional and climatic controls on seasonal dust deposition in the southwestern U.S. *Aeolian Research*, *3*(1), 3–21. https://doi.org/10.1016/j.aeolia.2011.03.008

Reynolds, R. L., Yount, J. C., Reheis, M., Goldstein, H., Chavez, P. Jr., Fulton, R., … Forester, R. M. (2007). Dust emission from wet and dry playas in the Mojave Desert, USA. *Earth Surface Processes and Landforms*, *32*(12), 1811–1827. https://doi.org/10.1002/esp

Reynolds, R. L., Munson, S. M., Fernandez, D., Goldstein, H. L., & Neff, J. C. (2016). Concentrations of mineral aerosol from desert to plains across the central Rocky Mountains, western United States. *Aeolian Research*, *23*, 21–35. https://doi.org/10.1016/j.aeolia.2016.09.001

Rivera Rivera, N. I., Gill, T. E., Bleiweiss, M. P., & Hand, J. L. (2010). Source characteristics of hazardous Chihuahuan Desert dust outbreaks. *Atmospheric Environment*, *44*(20), 2457–2468. https://doi.org/10.1016/j.atmosenv.2010.03.019

Routson, C. C., Overpeck, J. T., Woodhouse, C. A., & Kenney, W. F. (2016). Three millennia of southwestern north American dustiness and future implications. *PLoS One*, *11*(2), e0149573–e0149512. https://doi.org/10.1371/journal.pone.0149573

Saxton, K., Chandler, D., Stetler, L., Lamb, B., Claiborn, C., & Lee, B.-H. (2000). Wind erosion and fugitive dust fluxes on agricultural lands in the Pacific Northwest. *Transactions of ASAE*, *43*(3), 631–640. https://doi.org/10.13031/2013.2743

Schneider, E., Hajjeh, R. A., Spiegel, R. A., Jibson, R. W., Harp, E. L., Marshall, G. A., … Werner, S. B. (1997). A coccidioidomycosis outbreak following the Northridge, Calif, earthquake. *JAMA*, *277*(11), 904–908. https://doi.org/10.1001/jama.277.11.904

Seager, R., Harnik, N., Kushnir, Y., Robinson, W. A., & Miller, J. (2003). Mechanisms of hemispherically symmetric climate variability. *Journal of Climate*, *16*(18), 2960–2978. https://doi.org/10.1175/1520-0442(2003)016%3C2960:MOHSCV%3E2.0.CO;2

Seager, R., Harnik, N., Robinson, W. A., Kushnir, Y., Ting, M., Huang, H.-P., & Velez, J. (2005). Mechanisms of ENSO-forcing of hemispherically symmetric precipitation variability. *Quarterly Journal of the Royal Meteorological Society*, *131*, 1–28. https://doi.org/10.1256/qj.04.n

Seager, R., & Vecchi, G. (2010). Greenhouse warming and the 21st century hydroclimate of southwestern North America. *Proceedings of the National Academy of Sciences*, *107*(50), 21,277–21,282. https://doi.org/10.1073/pnas.0910856107

Sen, P. K. (1968). Estimates of the regression coefficient based on Kendall's Tau. *Journal of the American Statistical Association*, *63*(324), 1379–1389. https://doi.org/10.2307/2285891

Sheppard, P. R., Comrie, A. C., Packin, G. D., Angersbach, K., & Hughes, M. K. (2002). The climate of the US Southwest. *Climate Research*, *21*, 219–238. https://doi.org/10.3354/cr021219

Skiles, S. M., Painter, T. H., Belnap, J., Holland, L., Reynolds, R. L., Goldstein, H. L., & Lin, J. (2015). Regional variability in dust-on-snow processes and impacts in the Upper Colorado River Basin. *Hydrological Processes*, *29*(26), 5397–5413. https://doi.org/10.1002/hyp.10569

Swain, D., Horton, D. E., Singh, D., & Diffenbaugh, N. S. (2016). Trends in atmospheric patterns conducive to seasonal precipitation and temperature extremes in California. *Science Advances*, *2*(4), e1501344. https://doi.org/10.1126/sciadv.1501344

Swain, D. L., Tsiang, M., Haugen, M., Singh, D., Charland, A., Rajaratnam, B., & Diffenbaugh, N. S. (2014). The extraordinary California drought of 2013/2014: Character, context, and the role of climate change. *Bulletin of the American Meteorological Society*, *95*(9), S1–S104. https://doi.org/10.1175/1520-0477-95.9.S1.1

Tanaka, T. Y., & Chiba, M. (2006). A numerical study of the contributions of dust source regions to the global dust budget. *Global and Planetary Change*, *52*(1-4), 88–104. https://doi.org/10.1016/j.gloplacha.2006.02.002

Taylor, M. H., Losch, M., Wenzel, M., & Schröter, J. (2013). On the sensitivity of field reconstruction and prediction using empirical orthogonal functions derived from Gappy data. *Journal of Climate*, *26*(22), 9194–9205. https://doi.org/10.1175/JCLI-D-13-00089.1

Taylor, S. R., & McLennan, S. M. (1985). *The continental crust: Its composition and evolution*. Palo Alto, CA: Blackwell Scientific Pub.

Theobald, D. M., Travis, W. R., Drummond, M. A., & G. E. S. (2013). The changing Southwest. In G. Garfin et al. (Eds.), *Assessment of climate change in the Southwest United States: A report prepared for the National Climate Assessment*, (pp. 37–55). Washington, DC: Island Press. https://doi.org/10.5822/978-1-61091-484-0_3

Tong, D. Q., Wang, J. X. L., Gill, T. E., Lei, H., & Wang, B. (2017). Intensified dust storm activity and Valley fever infection in the southwestern United States. *Geophysical Research Letters*, *44*, 4304–4312. https://doi.org/10.1002/2017GL073524

Törnros, T., & Menzel, L. (2014). Addressing drought conditions under current and future climates in the Jordan River region. *Hydrology and Earth System Sciences*, *18*(1), 305–318. https://doi.org/10.5194/hess-18-305-2014

Tsang, C. A., Vugia, D. J., Benedict, K., Chiller, T., & Park, B. J. (2013). Increase in reported coccidioidomycosis—United States, 1998–2011. *Morbidity and Mortality Weekly Report*, *32*(11), 1237–1239. https://doi.org/10.1097/INF.0b013e31829e7a5c

Uno, I., Wang, Z., Chiba, M., Chun, Y. S., Gong, S. L., Hara, Y., … Westphal, D. L. (2006). Dust model intercomparison (DMIP) study over Asia: Overview. *Journal of Geophysical Research*, *111*, D12213. https://doi.org/10.1029/2005JD006575

Urban, F. E., Reynolds, R. L., & Fulton, R. (2009). The dynamic interaction of climate, vegetation, and dust emission, Mojave Desert, USA. In A. Fernandez-Bernal & M. A. De La Rosa (Eds.), *Arid environments and wind erosion*. NOVA Science Publishers.

VanCuren, R. A., & Cahill, T. A. (2002). Asian aerosols in North America: Frequency and concentration of fine dust. *Journal of Geophysical Research*, *107*(D24), 4804. https://doi.org/10.1029/2002JD002204

Vicente-Serrano, S. M., Beguería, S., & López-Moreno, J. I. (2010). A multiscalar drought index sensitive to global warming: The standardized precipitation evapotranspiration index. *Journal of Climate*, *23*(7), 1696–1718. https://doi.org/10.1175/2009JCLI2909.1

Wang, R., Balkanski, Y., Boucher, O., Bopp, L., Chappell, A., Ciais, P., … Tao, S. (2015). Sources, transport and deposition of iron in the global atmosphere. *Atmospheric Chemistry and Physics*, *15*(11), 6247–6270. https://doi.org/10.5194/acp-15-6247-2015

Wang, S., Huang, J., He, Y., & Guan, Y. (2014). Combined effects of the Pacific Decadal Oscillation and El Niño–Southern Oscillation on Global Land Dry–Wet Changes. *Scientific Reports*, *4*(1), 6651. https://doi.org/10.1038/srep06651

Webb, N. P., Herrick, J. E., Van Zee, J. W., Courtright, E. M., Hugenholtz, C. H., Zobeck, T. M., … Wagner, L. (2016). The National Wind Erosion Research Network: Building a standardized long-term data resource for aeolian research, modeling and land management. *Aeolian Research*, *22*, 23–36. https://doi.org/10.1016/j.aeolia.2016.05.005

Weiss, J. L., Castro, C. L., & Overpeck, J. T. (2009). Distinguishing pronounced droughts in the southwestern united states: Seasonality and effects of warmer temperatures. *Journal of Climate*, *22*(22), 5918–5932. https://doi.org/10.1175/2009JCLI2905.1

Wells, K. C., Witek, M., Flatau, P., Kreidenweis, S. M., & Westphal, D. L. (2007). An analysis of seasonal surface dust aerosol concentrations in the western US (2001–2004): Observations and model predictions. *Atmospheric Environment*, *41*(31), 6585–6597. https://doi.org/10.1016/j.atmosenv.2007.04.034

Yu, H., Remer, L. A., Chin, M., Bian, H., Kleidman, R. G., & Diehl, T. (2008). A satellite-based assessment of transpacific transport of pollution aerosol. *Journal of Geophysical Research*, *113*, D14S12. https://doi.org/10.1029/2007JD009349

Yu, H., Remer, L. A., Chin, M., Bian, H., Tan, Q., Yuan, T., & Zhang, Y. (2012). Aerosols from overseas rival domestic emissions over North America. *Science*, *337*(6094), 566–569. https://doi.org/10.1126/science.1217576

Zender, C. S., & Kwon, E. Y. (2005). Regional contrasts in dust emission responses to climate. *Journal of Geophysical Research*, *110*, D13201. https://doi.org/10.1029/2004JD005501

Zhao, T. L., Gong, S. L., Zhang, X. Y., Blanchet, J.-P., McKendry, I. G., & Zhou, Z. J. (2006). A simulated climatology of Asian dust aerosol and its trans-Pacific transport. Part I: Mean climate and validation. *American Meteorological Society*, *19*(1), 88–103. https://doi.org/10.1175/JCLI3605.1